Tokamak Disruption Simulation: Progress toward Comprehensive Modeling

Carl Sovinec

Dept. of Engineering Physics,
University of Wisconsin-Madison

2018 International Sherwood Fusion Theory Conference

April 23-25, 2018

Center for Tokamak Transient Simulation

Thesis and Outline

Past efforts in modeling disruptions advanced understanding by isolating effects, but integrated modeling is needed for predictive simulations.

- Introduction
  - General description
  - Simulation objectives
- Disruption physics & computations
- Example case
- Prospects for integrated simulation
  - Physical modeling
  - Computation
- Conclusions

Introduction: Disruption is an unplanned loss of plasma confinement; macroscopic dynamics are involved.

- Disruption releases stored energy over a short period of time.
  - Thermal energy and energy in $\mathbf{B}_{pol}$ in ITER may be freed over ~1 ms and ~10s of ms, respectively.
  - ITER plasma will store > 500 MJ. (~100 kg of dynamite)
- Three concerns arise with disruption:

  1) Thermal loading, 2) EM loading, and 3) Runaway e^- generation
- Extreme conservatism is not an option.

  "Burning plasma operation in ITER will require … … small margins against each of the three major plasma operation limits and under conditions where the need for external stabilization of NTM and/or RWM MHD instabilities … … is anticipated," Hender, *et al.*, NF **47**, S128 (2007).

Disruptions initiate through varying sequences.

Sequences are described in Greenfield, Nazikian, *et al.*, "Workshop on Transients in Tokamak Plasmas," Sponsored by the U. S. Dept. of Energy, June 8-11, 2015.

Tearing mode sequence

Trigger

Adverse events

Disruption precipice

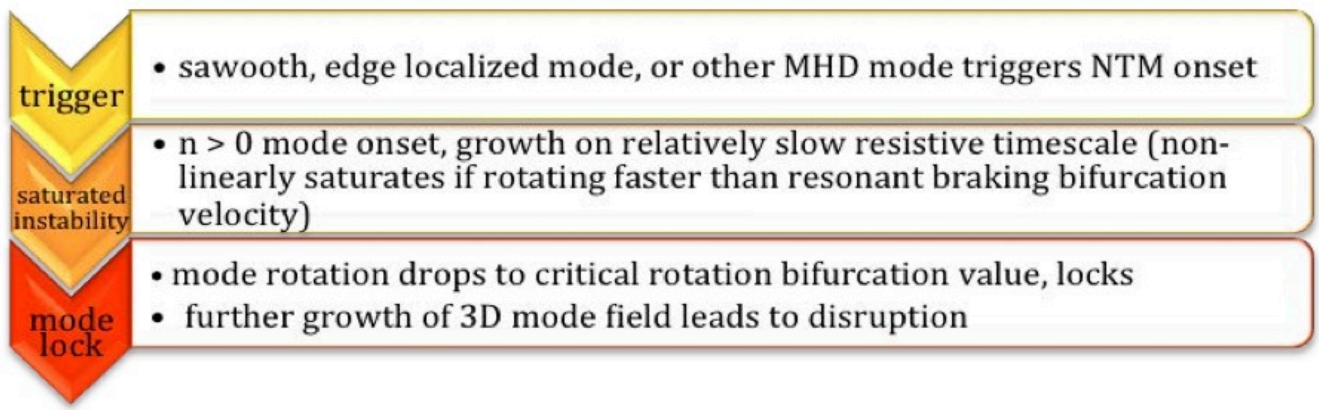

- Other sequences describe **VDE**, **global MHD**, **field error**, and **off-normal events**.

A fast thermal quench (TQ) preceding the current quench (CQ) is common.

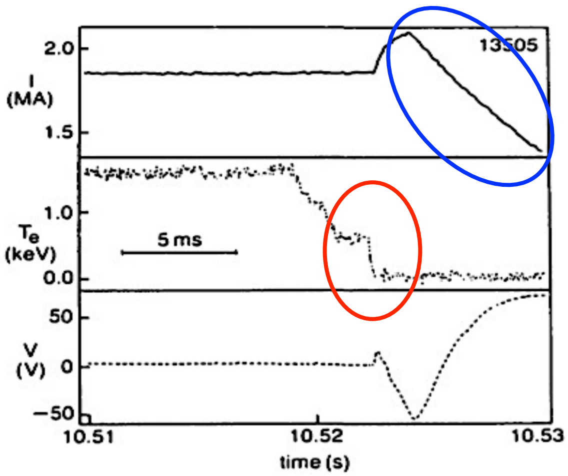

Density-limit disruption in limited JET. [Wesson, *et al*, NF **29**, 641 (1989)]

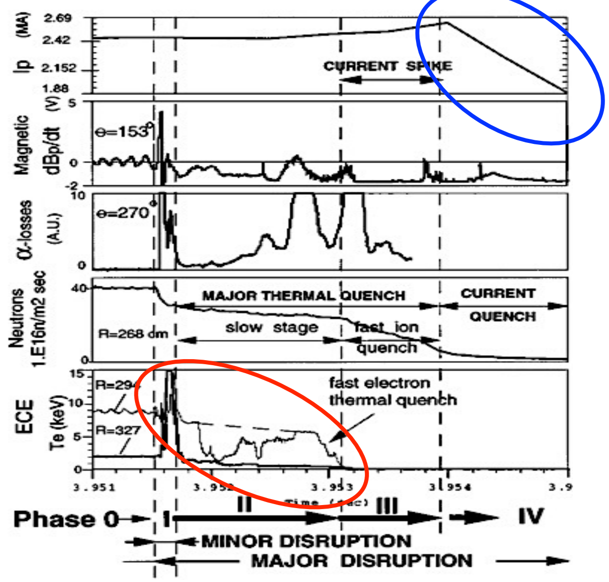

High-β disruption in TFTR. [Mirnov, *et al*, PoP **5**, 3950 (1998)]

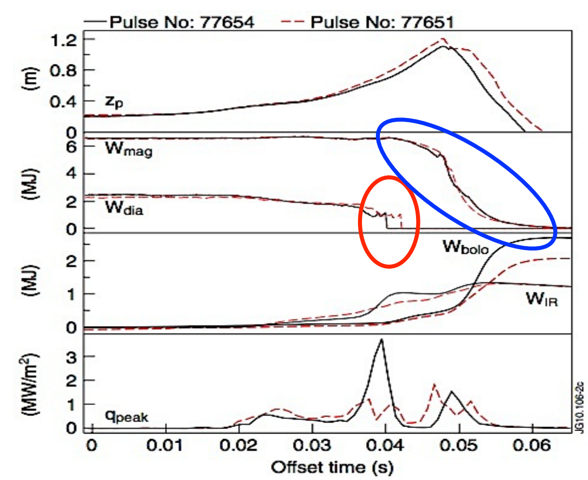

Forced VDE in diverted JET. [Riccardo, *et al*, PPCF **52**, 124018 (2010)]

- TQ is circled in red; CQ is circled in blue and extends off first two plots.

The propensity for disruption stems from a combination of properties.

- Linear stability alone does not provide a satisfying explanation.
  - Linear instability may not be problematic.
  - Nonlinear responses can limit consequences.

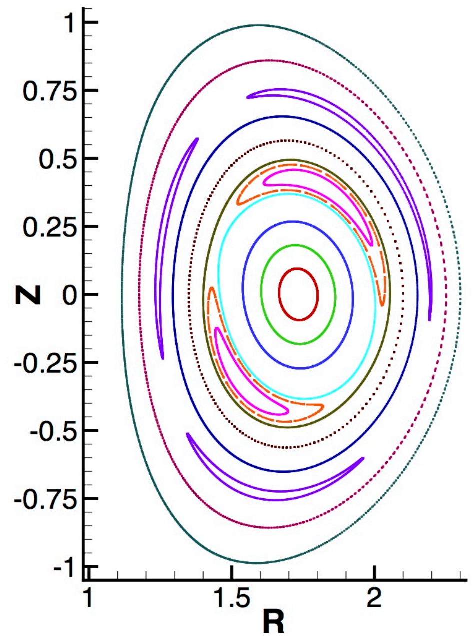

Nonlinearly saturated tearing, in itself, is not disruptive.

Relaxation analysis provides physical insights.

- First, consider relaxation of ideal, external kink.
  - Kadomtsev and Pogutse analyzed low-shear ideal columns [Sov-Phys-JETP **38**, 283 (1974)].
  - Minimizing potential energy leads to *bubble-swallowing* for $q_{\text{plasma}} < m/n$.
    - Conserve I_p, or
    - Flux of auxiliary field.
  - Fragmentation of the edge would affect edge confinement.

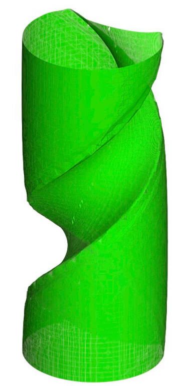

Relaxation analysis also provides insight for non-ideal evolution.

- The Taylor hypothesis conserves global magnetic helicity while minimizing magnetic energy [PRL **33**, 1139 (1974)].
  - The resulting states are equilibria with $\mathbf{J} = \lambda \mathbf{B}$ and uniform λ.
  - Apply to tokamak disruption by flattening *P* and $dF/d\psi$ while maintaining Φ and relative helicity.

$$H_{rel} = \int_{plasma} (\mathbf{A} - \mathbf{A}_{vac}) \cdot (\mathbf{B} + \mathbf{B}_{vac})\, dVol$$

[Finn & Antonsen, Comments PPCF **9**, 111 (1985)]

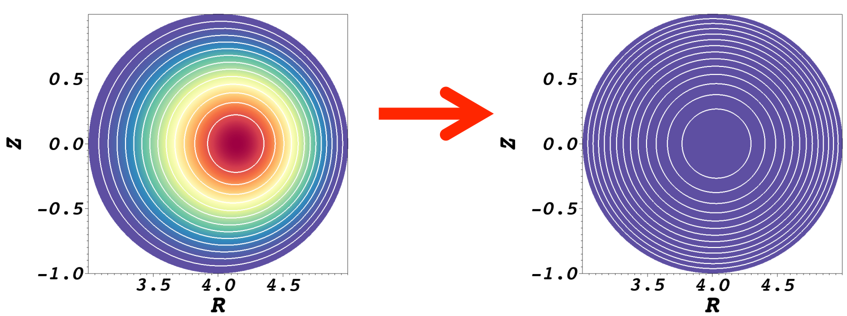

Circular, R/a = 4, β_{init}=5%; ψ and *P*.

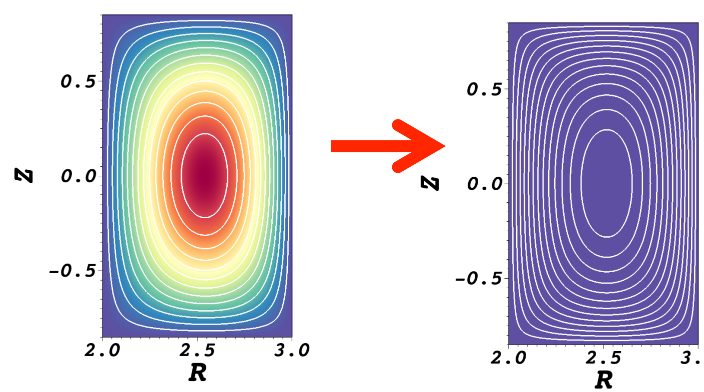

Rectangular, R/a = 2.5, β_{init}=10%; ψ and *P*.

Relaxation-induced changes in the *q*-profile imply disruptive consequences.

- Relaxation of tokamak current profiles flattens *q*, hence loss of shear.

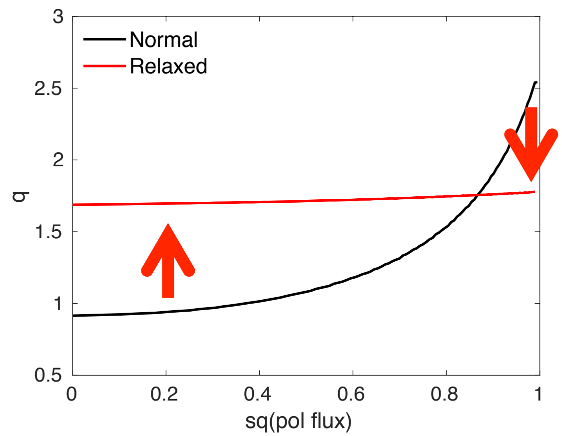

Effect on *q* for circular case.

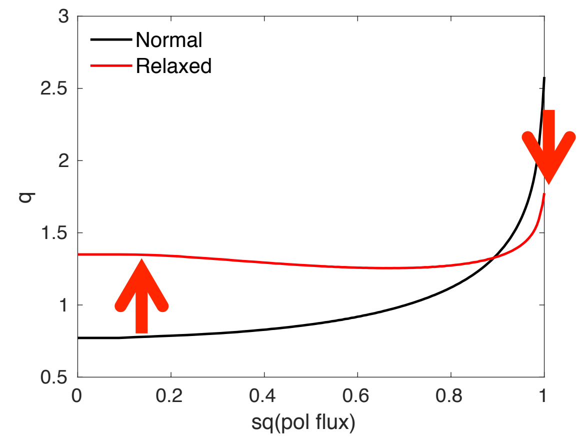

Effect on *q* for elongated rectangular case.

- Loss of magnetic shear implies:
  - Increasing island widths, $W = 4\sqrt{q_s\tilde{\psi}/|q_s' B_\theta|}$,
  - Increased susceptibility to external kink, depending on final *q*(*a*), and
  - Possible concurrent destabilization of ballooning.

Disruptive tokamak "relaxation" can be contrasted with the reversed-field pinch (RFP), where events are relatively benign.

- The same form of relaxation in the RFP increases magnetic shear.

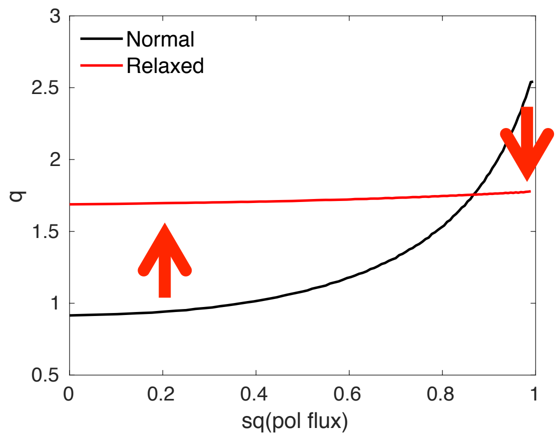

Effect on q for tokamak case.

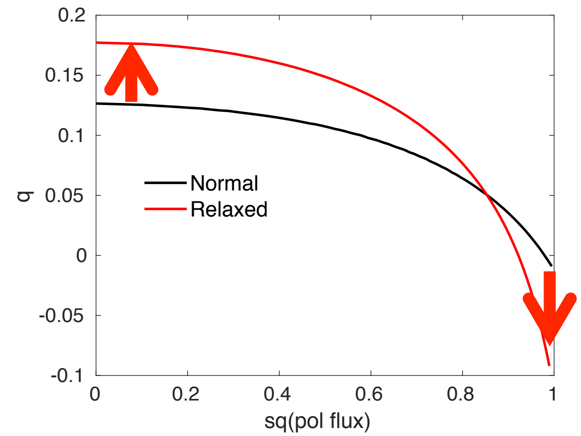

Effect on q for RFP case.

- Also, tokamak current profiles are sensitive to transport.
    - Tokamak peaked $J(\mathbf{x})$ stems from current drives and $\eta(T)$.
    - Loss of thermal energy affects $\eta(T)$.

There are two primary objectives for conducting numerical simulations of disruption.

1. Characterization of multi-physics transients
   - Macrosopic dynamics
   - External electromagnetics
   - Plasma and impurity transport
   - Runaway e^{-} generation
   - Plasma-surface interaction
   - Radiation
2. Practical modeling for addressing specific questions
   - Assessing wall forces
   - Engineering mitigation systems

[Bonoli, Curfman McInnes, *et al*, "Report of the Workshop on Integrated Simulations for Magnetic Fusion Energy Sciences," Sponsored by the U. S. Dept. of Energy, June 2-4, 2015.]

Disruption Physics and Simulation: Previous simulation studies investigated dynamics associated with disruption.

- External kink
- Resistive-wall mode
- Ballooning
- Vertical displacement
- Magnetic islands
- Runaway electron (RE) generation
- Impurity mixing for mitigation

Current-driven external kink places an operational limit on edge-*q*.

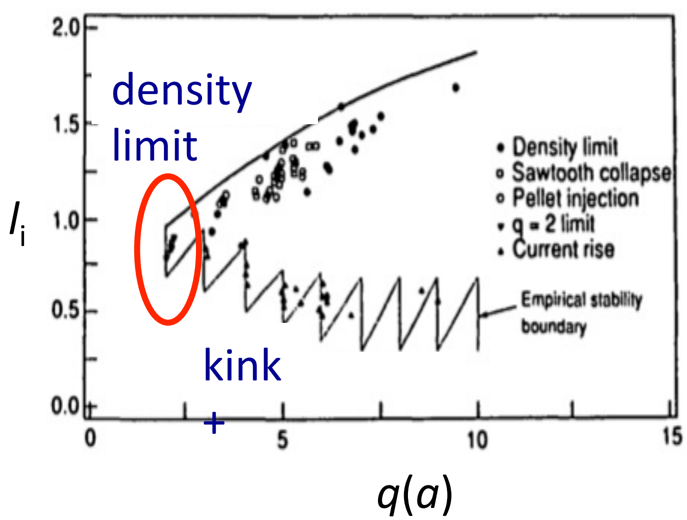

Edge-*q* / internal inductance operating space for limited JET. [Wesson, NF **29**]

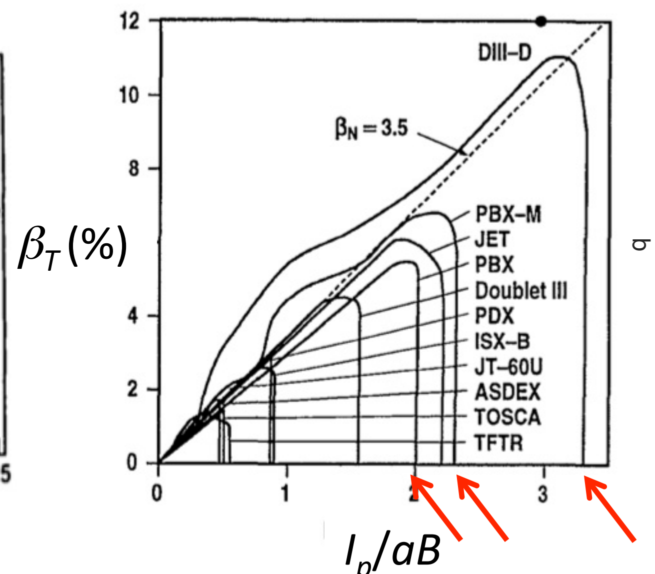

Current-driven kink is the upper limit on β-scaling results. [Strait, PoP **1**, 1415 (1994)]

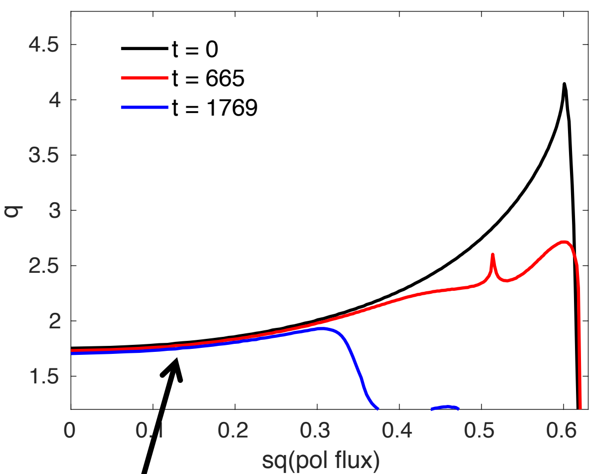

Computed *q*-profile evolution for a VDE.

- This limit can also be reached due to wall contact during disruption.

Basic cylindrical configurations verify external kink response.

- Rosenbluth, Monticello, Strauss, and White's reduced computation reproduced Kadomtsev and Pogutse's bubble swallowing [Phys Fluids **19**, 1987 (1976)].
- This problem has since been used as a nonlinear test for full MHD models.

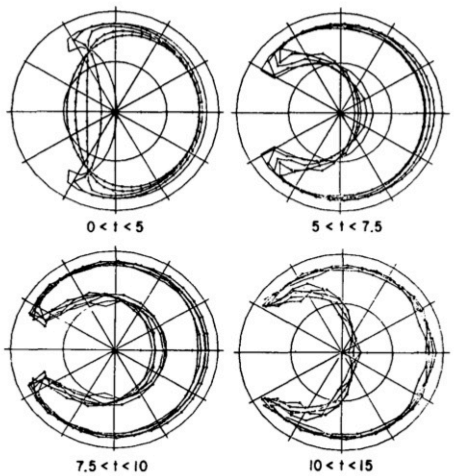

Reduced surface-tracking computation from RMSW.

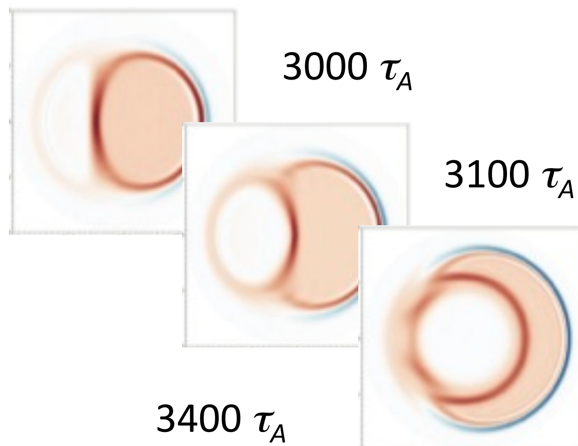

Axial current density from M3D [Breslau, PoP **22**, 062506 (2015)]

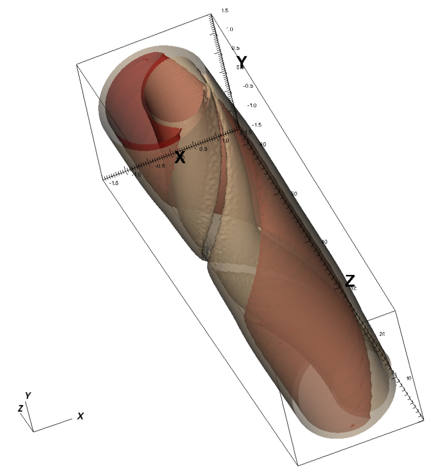

Particle density isosurfaces at 25% (tan) and 75% (red) of max from a NIMROD computation.

Kink dynamics are important for horizontal forcing during disruption.

- Horizontal forcing is described by Noll's relation [e.g., Riccardo, Noll, and Walker, NF **40**, 1805 (2000)]

  $$F_x = \pi B_\phi I_p \delta z_p$$

- Zakharov examined surface-contact destabilization in PoP **15**, 062507 (2008): "wall-touching kink mode."
- Zakharov, Galkin and Gerasimov applied "Tokamak MHD" to model coherent distortion of the entire plasma [PoP **19**, 055703 (2012)].
  - Based on time-scale separation, inertia is replaced by a relaxation parameter.
  - Low-order force-balance on distorting toroidal surfaces is maintained [PoP **22**, 062511 (2015)].

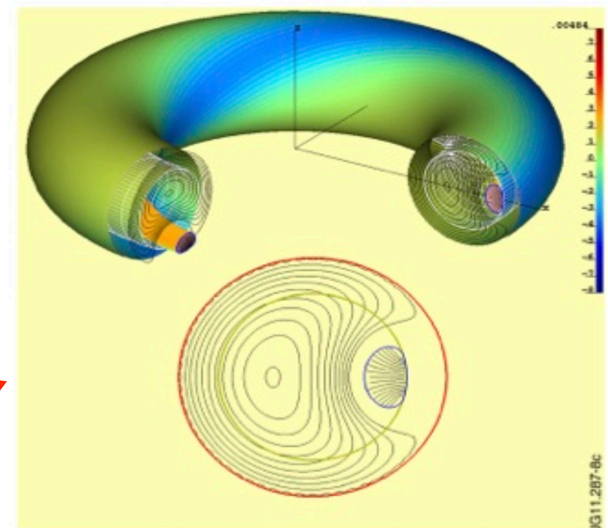

TMHD result on WTKM from the Disruption Simulation Code (DSC).

The no-wall Troyon β-limit is extended by a <u>resistive wall</u> in the presence of rotation and damping or kinetic effects.

- Limit is ideal-plasma pressure-driven instability [Troyon, *et al*, PPCF **26**, 209 (1984)].
- Rotation with damping (or kinetics) couples plasma and wall modes. [Bondeson and Ward, PRL **72**, 2709 (1994)].

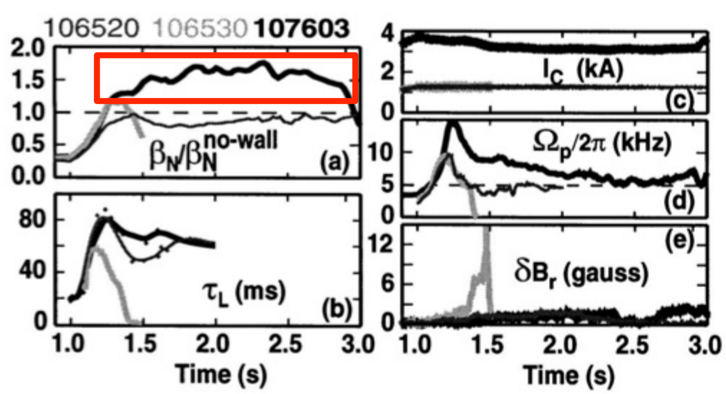

Rotation with field-error correction yields β_N~$1.5\beta_N^{\text{no wall}}$ in DIII-D [Garofalo, *et al*, PRL **89**, 235001 (2002)].

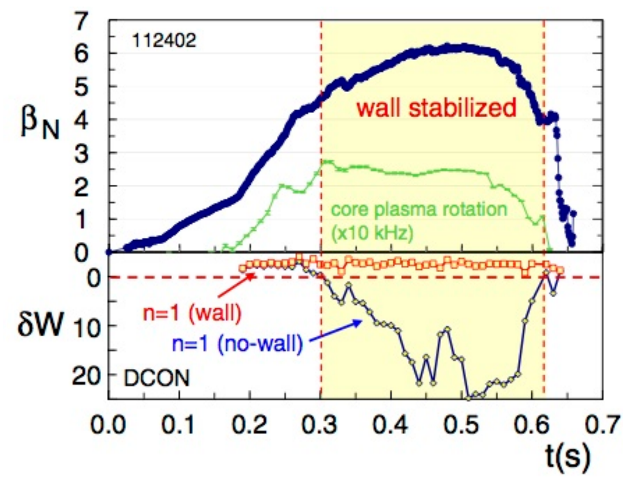

High β_N in this NSTX is ended by tearing-induced braking [Sabbagh, *et al*, NF **46**, 635].

Linear computation has contributed to RWM understanding, but nonlinear effects are largely unexplored.

- Besides Bondeson and Ward, Fitzpatrick and Aydemir [NF **36**, 11 (1996)] used analytics and linear computation.
- Berkery and coauthors have applied linear computation to study and validate kinetic effects [e.g., PRL **104**, 035003 (2010)].
- Recent nonlinear work with the JOREK is in [McAdams, et al, EUROFUSION WP15ER-PR(15)27].

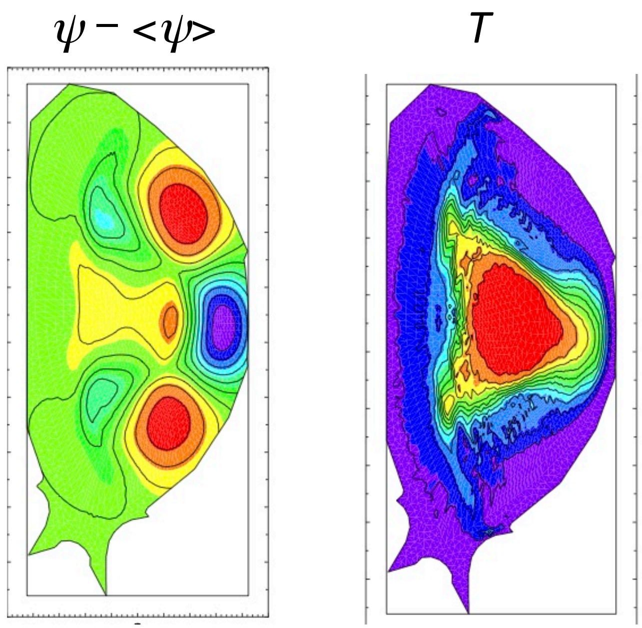

Strauss applied M3D to study nonlinear evolution of RWMs in ITER. [20th IAEA, TH2/2 (2004)]

<u>Ballooning</u> also leads to disruption.

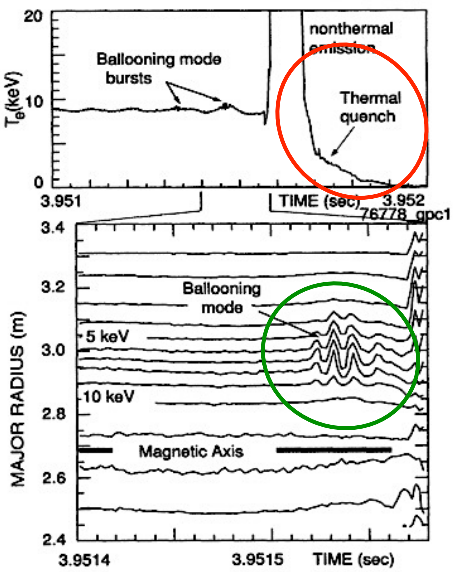

TFTR ECE signals suggest ballooning.

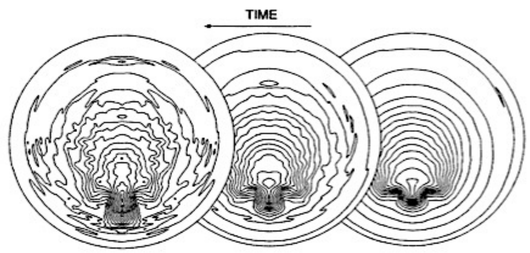

Localized pressure ballooning computed by MH3D.

- Park, *et al.* found ballooning as a disruptive secondary instability of internal kink in high-β TFTR discharges [PRL **75**, 1763 (1995)].

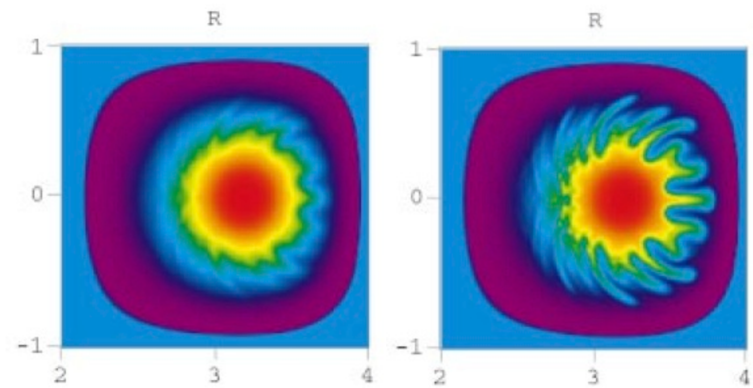

- Kleva and Guzdar investigated nonlinear mixing in resistive-MHD computations [PoP **8**, 103 (2001)].

<u>Vertical displacement</u> of the entire plasma column is common during disruption.

- Tokamaks rely on feedback to maintain positioning of elongated equilibria.
- Vertical displacement event (VDE) time-scale is set by the wall diffusion time, and $\tau_{MHD} \ll \tau_{wall} \ll \tau_{\eta}$.
- 2D computations of VDE approximate force-balance.
  - Toroidal simulation code [Jardin, *et al.* JCP **66**, 481 (1986)].
  - DINA [Khayrutdinov and Lukash, JCP **109**, 193 (1993)].

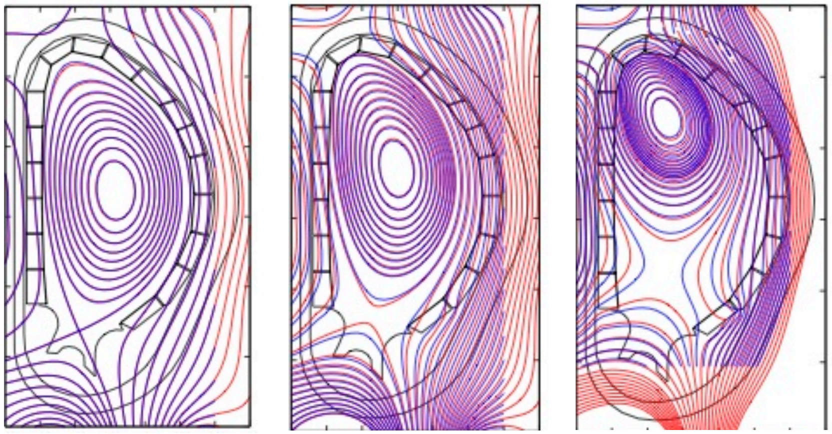

Comparison of TSC (blue) and DINA (red) evolution of ITER flux surfaces over 16 ms, including vacuum vessel and blanket modules [Miyamoto, *et al,* NF **54**, 083002 (2014)].

Three-dimensional computations allow vertical motion with asymmetry.

- Strauss, *et al.* conducted the first 3D simulations by coupling the M3D code to a resistive boundary model [CPC **164**, 40 (2004)].
- Paccagnella, *et al.* applied the model to predict toroidal current peaking in ITER [NF **49**, 035003 (2009)].
- Strauss, *et al.* found maximum wall forcing at $\gamma\tau_{\mathrm{w}} \sim 1$ [PoP **17**, 082505 (2010); PoP **22**, 082509 (2015)].

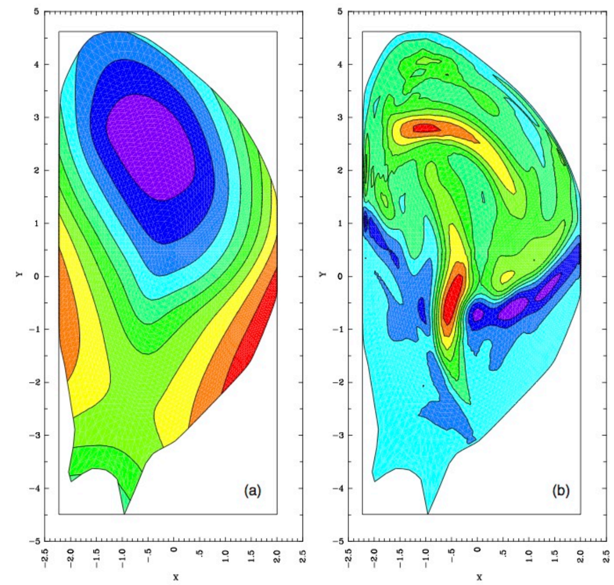

Poloidal flux (left) and $-RJ_{\phi}$ (right) from Strauss, *et al.* (2010) starting from a vertically unstable ITER equilibrium rescaled to kink.

Recent computations with the M3D-C[1] code examine edge instability from a VDE in NSTX.

- Pfefferlé, *et al.* model NSTX discharge 132859, where feedback was turned off [PoP **26**, 056106 (2018)].
- Nonlinear kink instability develops when $q(a)$ decreases below 2.
- Magnetic chaos develops from the edge and leads to final TQ and CQ.

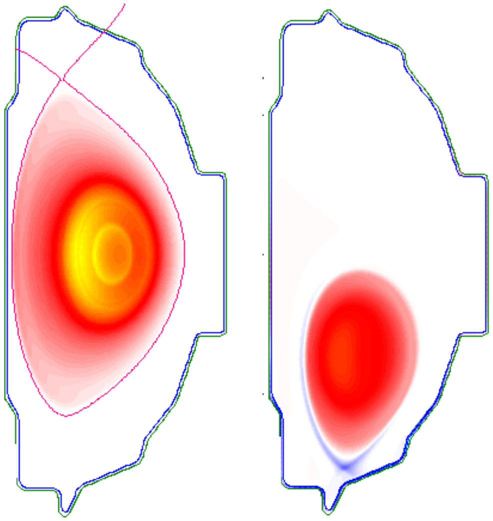

Contours of RJ_ϕ at t = 0 and at t = 7325 $\tau_{A.}$

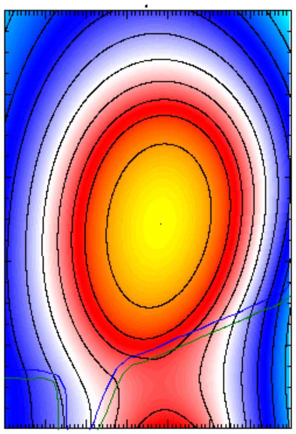

Poloidal flux ψ from 3D run at t=7825.

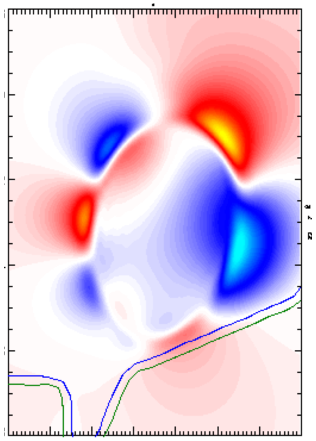

Kink is evident in $d\psi/d\phi$.

Figures courtesy of S. Jardin, N. Ferraro, and D. Pfefferlé.

Magnetic islands play an important role in disruption.

- Neoclassical island growth, flow-braking, and locking was the most frequent cause of disruption over a decade of JET operation [de Vries, *et al*, NF **51**, 053018 (2011)].

- Radiation in density-limit disruption destabilizes magnetic islands [Wesson, *et al*, NF **29**, 641 (1989); Gates, *et al*, PoP **22**, 060701 (2015)].

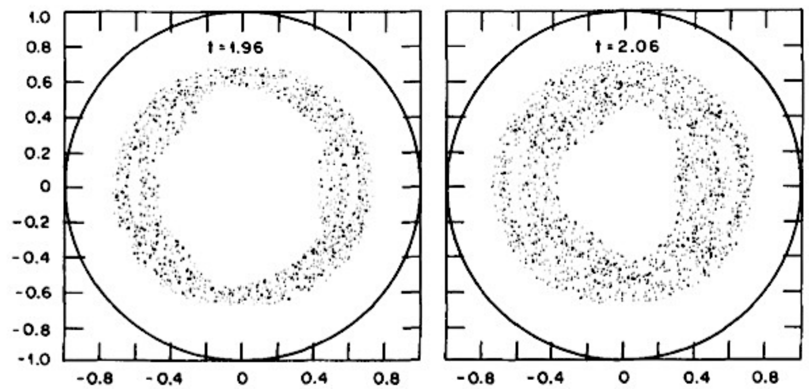

Carreras, Hicks, Homes, and Waddell computed 2/1 & 3/2 island overlap in conditions motivated by Princeton's PLT tokamak [PF **23**, 1811 (1980)].

Islands generated as a nonlinear consequence of ideal instability can also lead to disruption.

- Callen, *et al.*, analytically modeled the growth of ideal interchange subject to pressure evolution during heating with negative central shear [PoP **6**, 2963 (1999)].

- Kruger, *et al*., modeled the consequences with NIMROD and found disruptive heat loss resulting from the overlap of 2/1 and 3/1 magnetic islands [PoP **12**, 056113 (2005)].

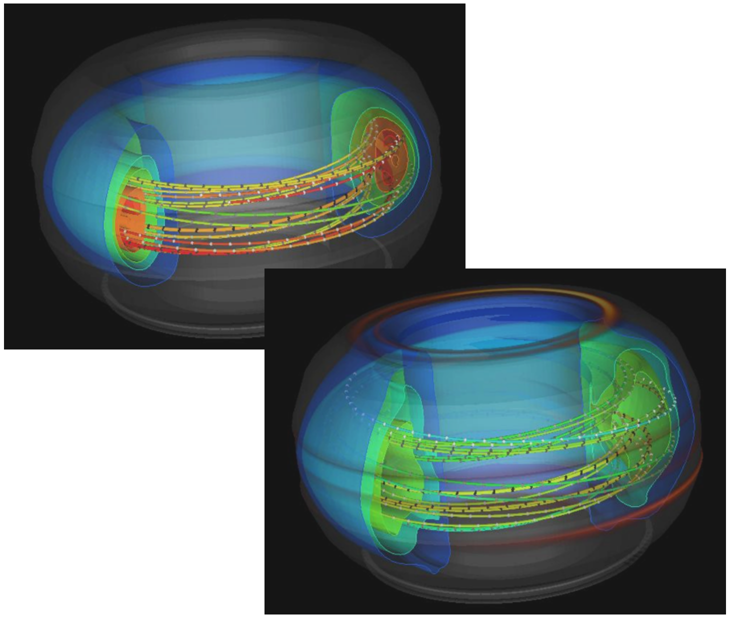

Overlap of 2/1 and 3/1 islands and chaotic edge lead to heat deposition in a simulation of DIII-D discharge 87009.

Island interaction with plasma flow affects stability.

- Fitzpatrick found bifurcation when balancing field-error induced EM torque and viscous torque in analogy to an induction motor [PoP **5**, 3325 (1998)].
- Bifurcation also occurs for tearing-unstable conditions [NF **33**, 1049 (1993)].
- Island-induced changes in flow affect RWM stability.

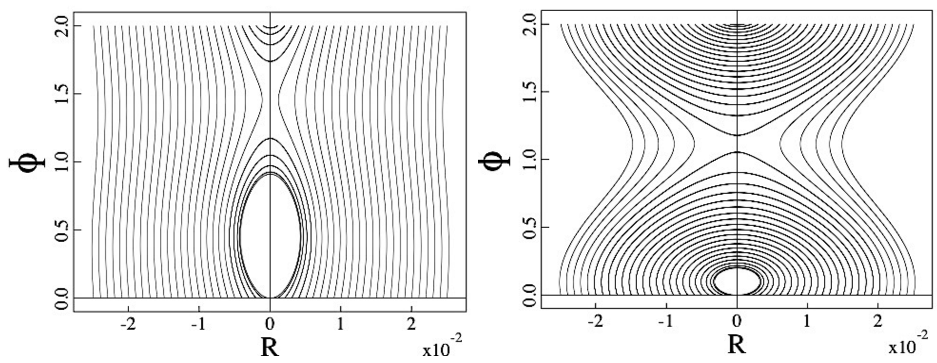

Computed magnetic islands for high-flow (left) and low-flow (right) states of a perturbed, linearly stable slab geometry configuration [Beidler, *et al*, PoP **24**, 052508 (2017); also, next talk].

Neoclassical effects are important for island evolution.

- Yu, *et al.* modeled NTM growth and saturation using a reduced cylindrical configuration with heuristic bootstrap current density:
  $j_{BS} \propto -\left(\varepsilon / B_{pol}\right) dp/dr$
  [PoP **5**, 3924 (1998)]

- Popov, *et al.* used the same relation in an MHD model of NTM seeding in DIII-D [PoP **9**, 4205 (2002)].

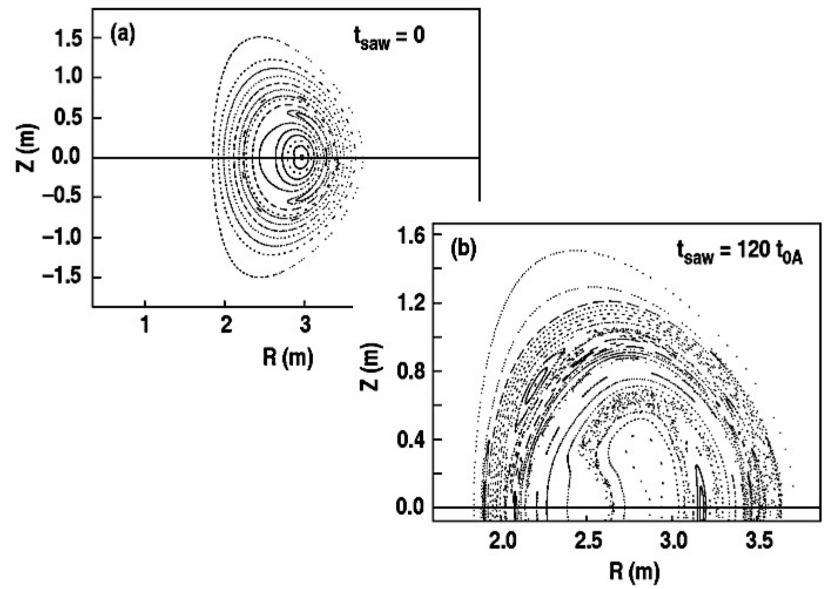

Sawtooth excitation of 2/2 and 3/2 in NFTC computation of DIII-D discharge 86144 [PoP **9**, 4205].

Runaway electron generation influences the CQ.

- More than 50% conversion of pre-disruption current can be converted to REs [Hender, NF **47**].
- Collimation of runaway current challenges vertical positioning control.

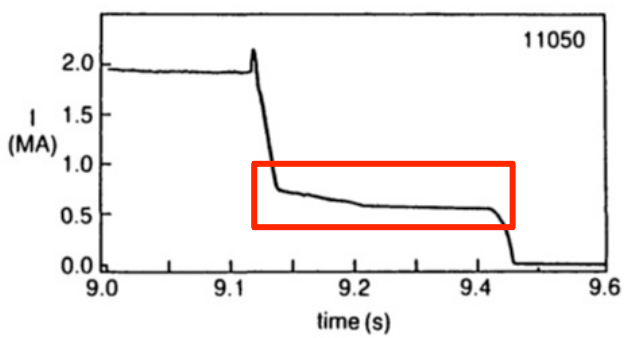

Current plateau from limited JET had resistance ~1/1000 of Spitzer [Wesson, NF **29**].

Soft X-ray imaging shows current channel in JET progressing toward divertor [Gill, NF **40**, 302 (2000)].

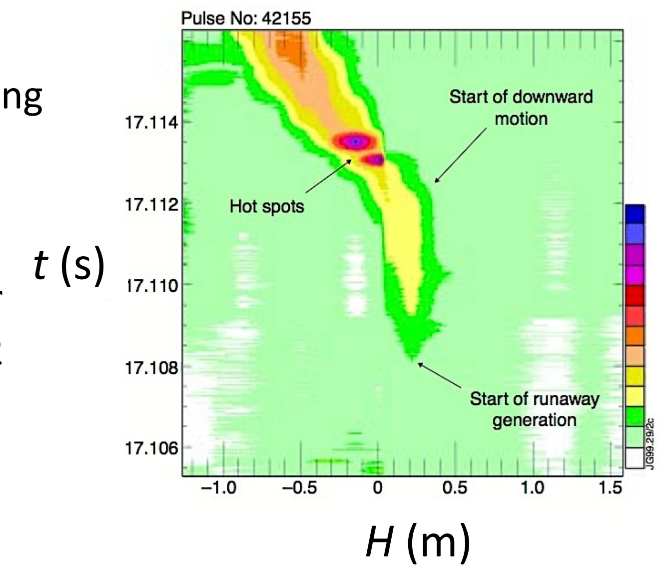

Theoretical studies examine the influences on RE evolution.

- Boozer [PoP **22**, 032504 (2015)] summarizes issues for ITER.
- Breizman describes stiff conditions associated with avalanche criticality [NF **54**, 072002 (2014)].
- Liu, *et al.* solve the adjoint FP equation for RE slowing with collisions and synchrotron radiation [PoP **23**, 010702 (2016)].
- Stahl, *et al.* evolve the distribution, numerically, including collisions, synchrotron radiation, and avalanche generation [NF **56**, 112009 (2016)].
- + + +
- Eriksson and Helander combined Monte Carlo FP with spatially 1D electromagnetics in ARENA [CPC **154**, 175 (2003)].

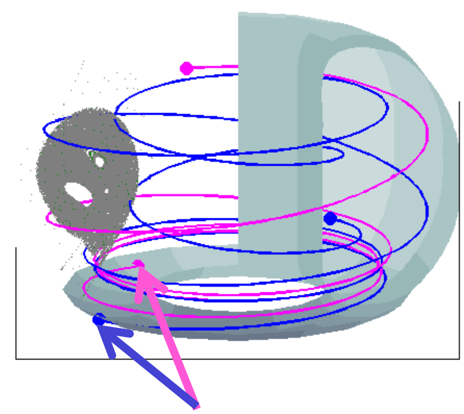

When magnetic fields become stochastic in NIMROD computations, REs escape, striking the outer divertor. [courtesy of V. Izzo]

- Izzo, *et al.* compared RE test-particle confinement with measured DIII-D RE current [PPCF **54**, 095002 (2012)].

Disruption mitigation systems provide last-resort protection.

- Izzo and Whyte integrated NIMROD and KPRAD to model massive gas injection (MGI) impurity mixing and radiation.
- Simulations show roles of MHD:
  - Simulated 2/1 island induced by edge cooling conducts heat out to impurities [NF **46**, 541 (2006)].
  - When 1/1 kink is also excited, it advects hot plasma into impurities [PoP **20**, 056107 (2008)].
  - Radiation asymmetry results from MHD, even with symmetric injection.

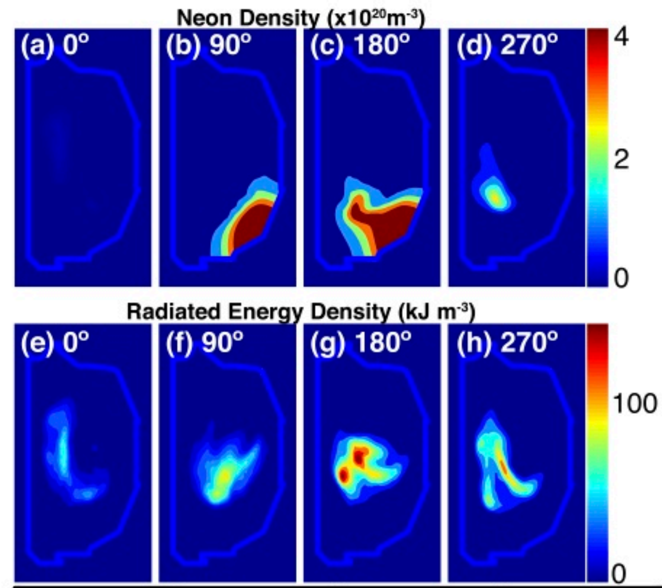

Eidietis, Izzo, and coauthors examine toroidal and poloidal radiation asymmetry, comparing DIII-D and simulated emission [PoP **24**, 102504 (2017)].

Example result: A recent computation demonstrates multiple disruption effects.

- The computation models forced vertical displacement.
- Model is full MHD with $\eta(T)$, anisotropic thermal conduction and viscous stress.
- Time-scales are separated:

$$\tau_\eta \sim 1000\ \tau_{\text{wall}} \sim 10^6\ \tau_A$$

Schematic of Configuration

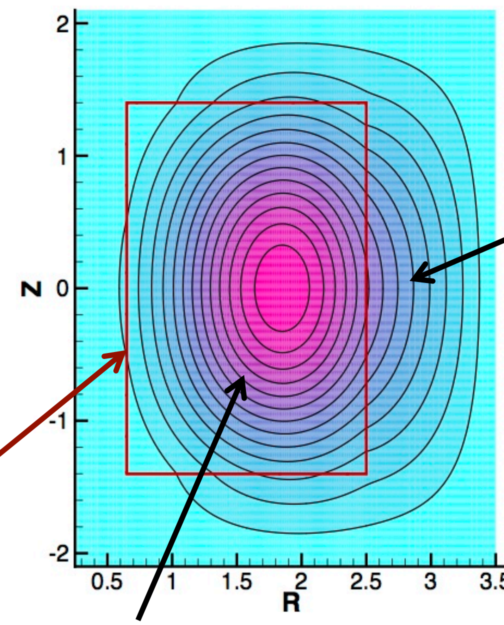

external region

resistive wall and other bc's

central region (subsequent plots)

The 3D computation described here starts from an up-down symmetric equilibrium.

- $\beta(0) \cong 1\%$
- $q(0) = 1.75$

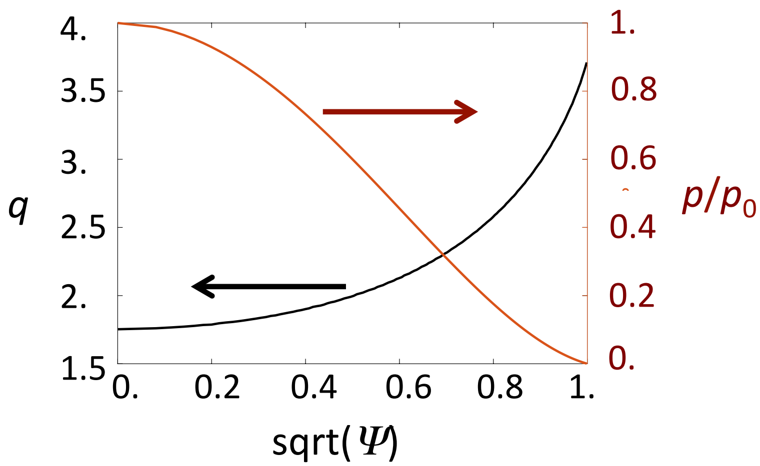

Safety factor and pressure profiles.

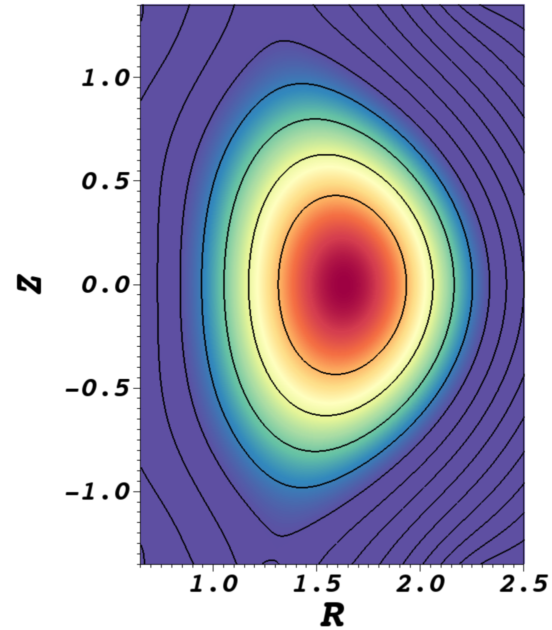

Contours of poloidal flux and pressure for the initial state.

- VDE is initiated by removing current from the upper divertor coil (outside the resistive wall).

Continuous MHD activity develops and evolves throughout the simulated transient.

- The dominant mode changes with increasing wall contact.

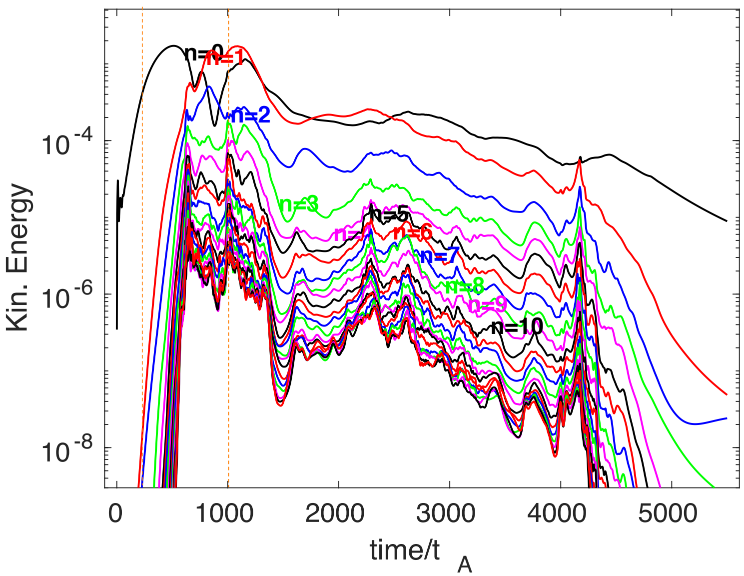

Kinetic energy fluctuations ($0 \leq n \leq 21$) indicates multiple events over time.

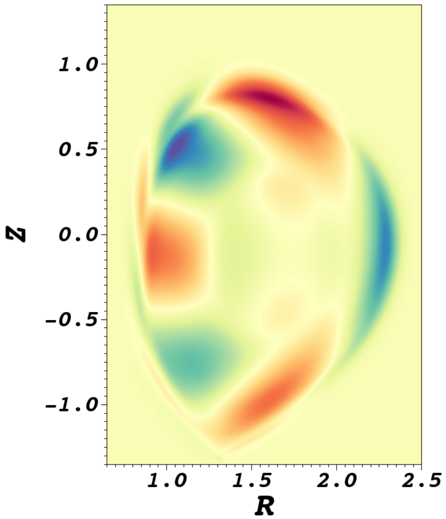

n = 1 pressure contours at t = 225 primarily shows m = 3.

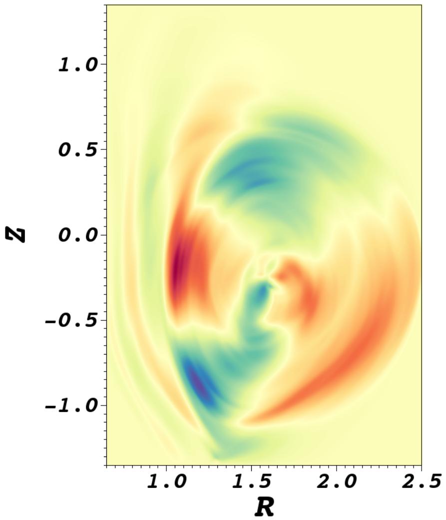

At t = 999, n = 1 perturbations are primarily m = 2.

The plasma shape is severely deformed near the peak in MHD activity.

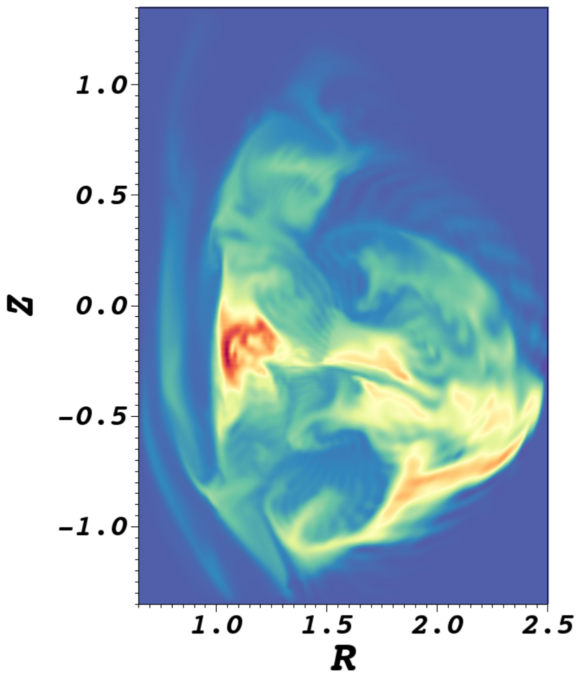

Pressure in the $\phi = 0$ plane at $t = 999$ indicates that the MHD has nearly inverted the initially peaked profile.

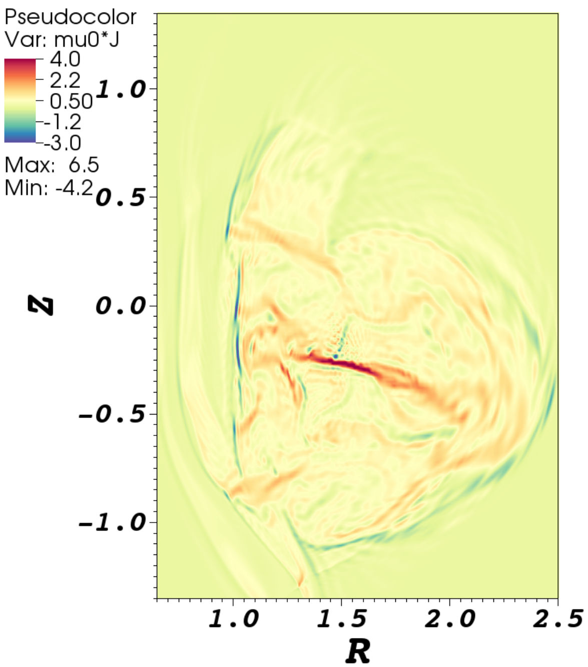

Parallel current density becomes filamented and stretched into sheets. [Plot shows $\lambda = \mu_0 J_{||}/B$ at $\phi = 0$ and $t = 999$.]

Global diagnostics show that plasma current persists longer, and energy confinement decreases faster, with toroidal asymmetry.

- The previous plots are at the beginning of a current spike and during the thermal quench.

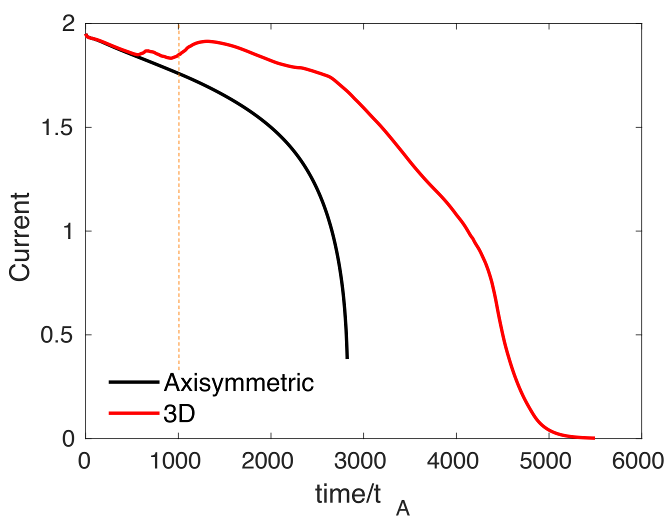

The current in the 3D computation spikes above the 2D result during the filamentation.

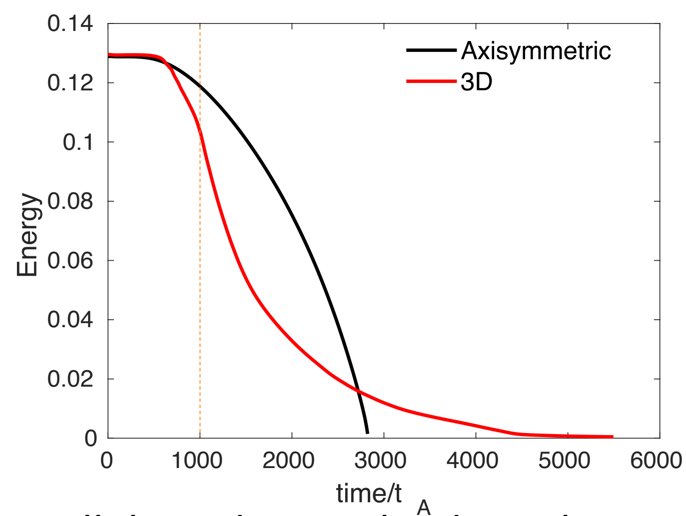

Parallel conduction leads to thermal quenching that is faster than the current quench.

Net horizontal forcing on the resistive wall results from the toroidal asymmetry.

- Plasma does not support net force, and plasma+wall is an electrically isolated system [Pustovitov, Nucl Fusion **55**, 113032].
- Computation of $F_j = \mu_0^{-1} \oint d\mathbf{S} \cdot \left[\mathbf{BB} - \underline{\underline{\mathbf{I}}} B^2/2 \right] \cdot \hat{\mathbf{e}}_j$ is over the outside of the resistive wall.

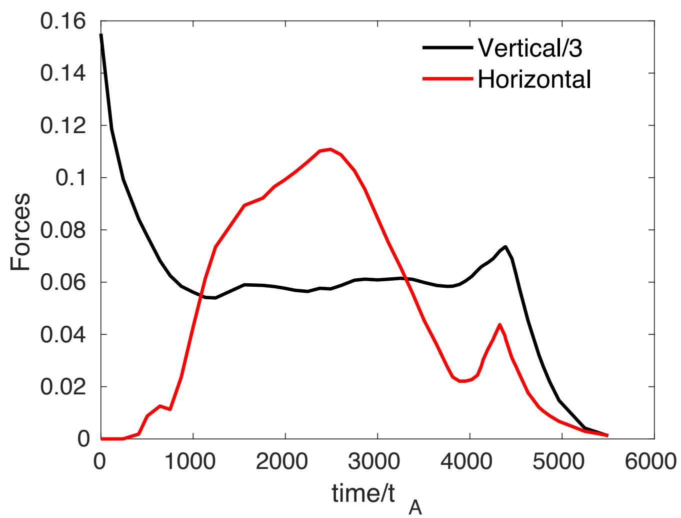

Horizontal forcing results from vertical I_p excursions crossing B_ϕ, supported by the wall.

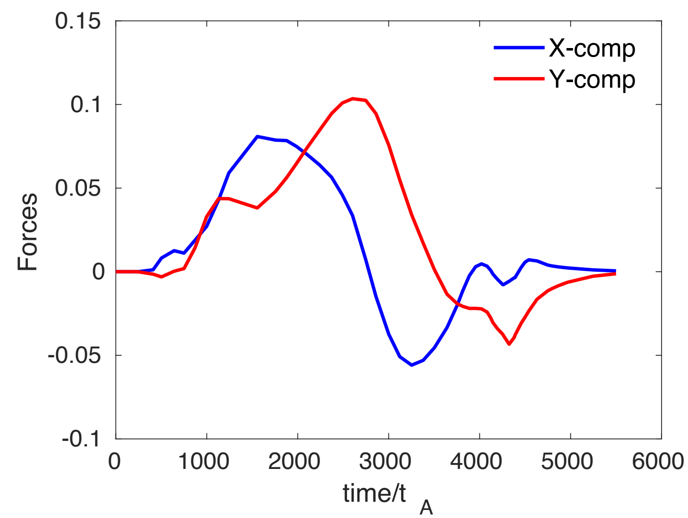

Cartesian components in the horizontal plane indicate slow rotation of the force.

While these efforts have been productive, we can read the classic elephant fable as cautioning against piecemeal modeling.

And so these men of Indostan
Disputed loud and long,
Each in his own opinion
Exceeding stiff and strong,
Though each was partly in the right,
And all were in the wrong!

from *The Blind Men and the Elephant* by John Godfrey Saxe

Blind monks examining an elephant: photo of ukiyo-e print by Hanabusa Itchō (1652–1724). [public domain art – wikipedia].

Prospects: An integrated model is needed to describe the interactions among physical effects during disruption.*

- Progress through isolating effects cannot remain the paradigm for disruption modeling.
- Assess prospects, here, by
  - Listing physical effects,
  - Weighing full vs. reduced modeling, and
  - Considering computational implications.

*Bonoli, Curfman McInnes, *et al*, "Report of the Workshop on Integrated Simulations for Magnetic Fusion Energy Sciences," Sponsored by the U. S. Dept. of Energy, June 2-4, 2015.

Organize physics list from the core outward.

1. Macroscopic dynamics with **B**-topology evolution
   - Island evolution and stochasticity
   - Kink and vertical displacement
   - Full / reduced / tokamak MHD
2. Kinetic-closure information
   - Perturbed bootstrap current for NTMs
   - Neoclassical viscosity for rotation damping
   - Parallel heat transport (TQ)
   - Cross-field transport
   - Fast-ion effects for RWMs
   - Coupled kinetics vs. reduced-model closures

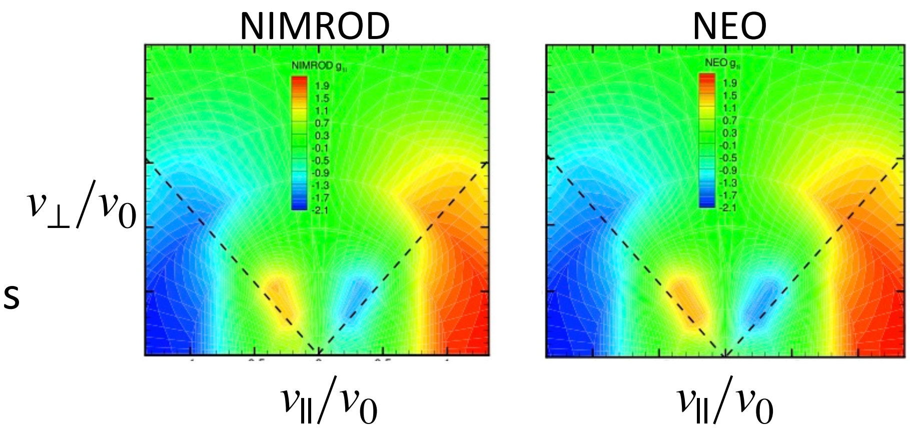

Drift-kinetic f_{ion} computed for a DIII-D like equilibrium [Held, *et al*, PoP **22**, 032511 (2015)].

Organize physics list from the core outward (cont).

3. Runaway-electron kinetics
   - Distribution and confinement
   - Macroscopic effects on η during CQ
4. Impurity flows and radiation
   - Density-limit physics & TQ
   - Mitigation (gas and pellets)
   - Neutrals and charged species
   - Reductions via fluid approximations
5. Plasma-surface interaction
   - Sheath effects on currents, energy, and flows
   - Impurity sourcing

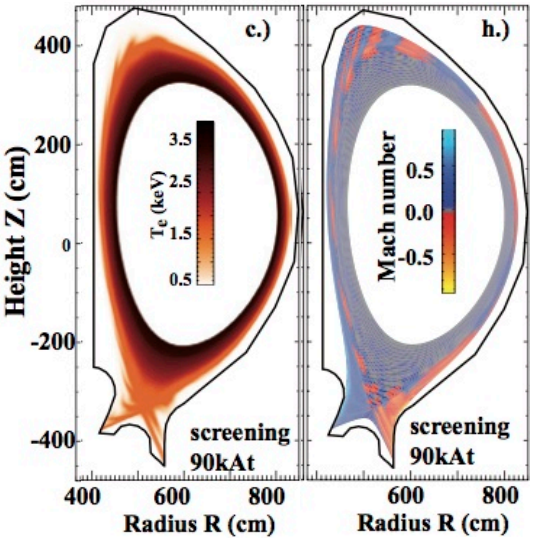

EMC3-EIRENE modeling of ITER 3D edge plasma and MC-neutral transport is magnetostatic [Schmitz, *et al*, NF **56**, 066008 (2016)].

Organize physics list from the core outward (cont).

6. External electromagnetics
   - RWM responses and field-error
   - Forcing from VDE and kink
   - Level of detail

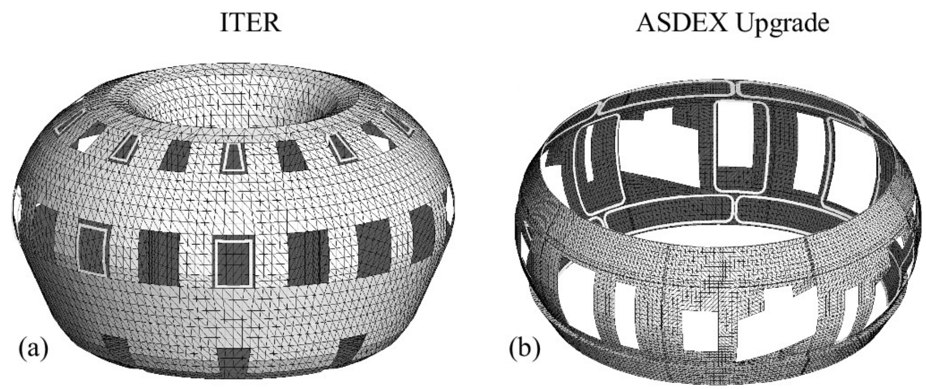

STARWALL/OPTIM models of resistive shells and feedback coils used in linear RWM computations [Strumberger, *et al*, PoP **15**, 056110 (2008)].

The numerical implications of an integrated model need equal consideration.

- Integrated disruption simulation is a *multiphysics* [Keyes, *et al.* IJHPC **27**, 4 (2013)] and *multiscale* application.
  - Multiple coupled effects
  - Macro- and micro-physics
  - Ranges of temporal and spatial scales
- The applied math side of the 2015 IS workshop offered sage advice:

  "… it is better to consider the complete collection of physics or scales at the outset and make informed choices … … about how to split or partition it than to start with a collection of models and try to determine how to glue them together." [Bonoli, Curfman McInnes, *et al*.]

Algorithm choices should be made by distinguishing tight and loose couplings.*

- This preliminary assessment does not represent directionality.
- How is coupling strength best quantified?

	Macro dynamics	Majority closure	RE physics	Impurity flow	PSI
Majority closure					
RE physics					
Impurity flow					
PSI					
Ext EM					

Darker shading indicates tighter coupling.

*Bonoli, Curfman McInnes, *et al.*

Developments in numerical methods will help the effort.

1. Asymptotic preserving methods [1]
2. Temporal integrators
   - IMEX for stiff systems [2]
   - High-order DIRK [3]
3. Linear and nonlinear algebraic-system solvers [4]
4. Vector elements and discontinuous Galerkin
5. Analysis and development for multiphysics problems [5]

[1] Degond and Deluzet, JCP **336**, 429 (2017)
[2] Kadioglu & Knoll, intechopen.com (2011)
[3] Najafi-Yazdi & Mongeau, JCP **233**, 315 (2013)
[4] Knoll & Keyes, JCP **193**, 357 (2004)
[5] Keyes, *et al.* IJHPC **27**, 4 (2013)

$$
\begin{tikzcd}
\mathcal{F}_\delta^\varepsilon \arrow[r, "\varepsilon \to 0"] \arrow[d, "\delta \to 0"] & \mathcal{F}_\delta^0 \arrow[d, "\delta \to 0"] \\
\mathcal{F}^\varepsilon \arrow[r, "\varepsilon \to 0"] & \mathcal{F}^0
\end{tikzcd}
$$

$\varepsilon \equiv$ small physics parameter

$\delta \equiv$ numerical discretization parameter

Conceptual schematic of asymptotic-preserving paradigm [Chacón, *et al*, JCP **272**, 719 (2014)].

We expect progress in computer hardware to bolster integrated simulation.

- Leadership class computing hardware is approaching *exascale* performance.
    - *Manycore* architectures extend parallelism at the expense of latency and single-thread performance [wikipedia.org].
    - *GPU* accelerators add performance but increase programming complexity.
- New architecture-aware libraries aim to relieve programmers of hardware-specific optimization [github.com/kokkos].

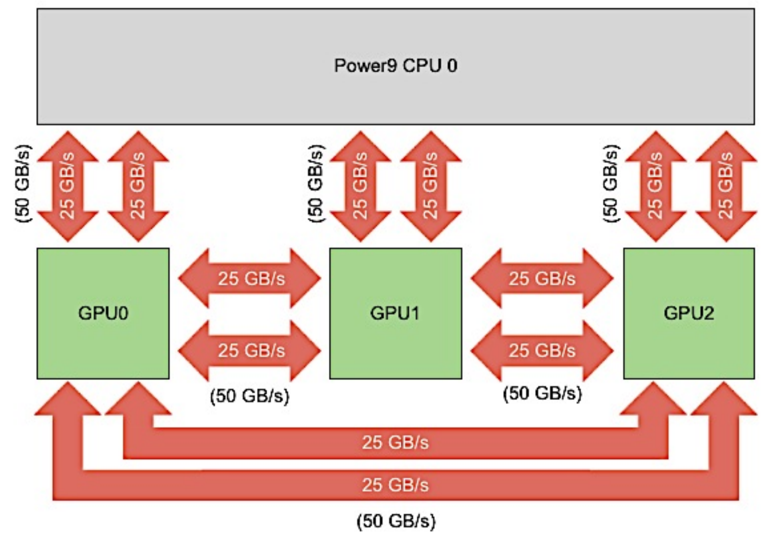

Intra-node connectivity on ½ of each of 4600 nodes on ORNL's new Summit system (~200 PF total) [orlc.ornl.gov].

We should be both optimistic and realistic about hardware advances.

- Developments are truly impressive.
  - Each node of Summit yields ~40 Tflops.
  - NERSC's entire Bassi system (Jan. 2006) was ~1/6 as fast.

- The multiscale nature of disruption physics includes propagation of information.
  - Implicit wave advances *and* elliptic potential/equilibrium solves communicate data.
  - Modern hardware favors flops over data movement.
- The multiphysics aspects of disruptions engender complex modeling.

Conclusions

- Reductionistic analysis has been productive for understanding fundamental effects.
- Recent, more comprehensive models are being applied to specific issues with disruption.
  - MHD + radiation ➔ mitigation
  - MHD + external electromagnetics ➔ wall forces
- While numerically challenging, integrated disruption simulation is needed to help tame the tokamak's elephant.

Our computations use visco-resistive (full) MHD with fluid closures.

$$\frac{\partial n}{\partial t}+\nabla\cdot\left(n\mathbf{V}\right)=\nabla\cdot\left(D_n\nabla n-D_h\nabla\nabla^2 n\right)$$

particle continuity with artificial diffusion

$$mn\left(\frac{\partial}{\partial t}+\mathbf{V}\cdot\nabla\right)\mathbf{V}=\mathbf{J}\times\mathbf{B}-\nabla(2nT)-\nabla\cdot\underline{\Pi}$$

momentum density

$$\frac{n}{\gamma-1}\left(\frac{\partial}{\partial t}T+\mathbf{V}\cdot\nabla T\right)=-nT\nabla\cdot\mathbf{V}-\nabla\cdot\mathbf{q}$$

temperature evolution

$$\frac{\partial\mathbf{B}}{\partial t}=-\nabla\times\left(\eta\mathbf{J}-\mathbf{V}\times\mathbf{B}\right)$$

Faraday's law & resistive MHD Ohm's

$$\mu_0\mathbf{J}=\nabla\times\mathbf{B}\qquad\qquad\nabla\cdot\mathbf{B}=0$$

Ampere's law and constraint

- The NIMROD code (https://nimrodteam.org) is used to solve linear and nonlinear versions of this system.

Closure relations approximate plasma transport effects.

- Magnetic diffusivity depends on temperature.
  - $\eta_0 \tau_A / \mu_0 a^2 \cong 1\times 10^{-6}$
  - $\eta(T) = \min\left[\eta_0 (T_0/T)^{3/2}\ ,\ 1\right]$
- Thermal conduction and viscous stress are anisotropic with fixed coefficients.
  - $\mathbf{q} = -n\left[(\chi_{\|} - \chi_{iso})\hat{\mathbf{b}}\hat{\mathbf{b}} + \chi_{iso}\underline{\mathbf{I}}\right]\cdot\nabla T\ ;\quad 0.075 \le \chi_{\|} \le 0.75,\quad \chi_{iso} = 7.5\times 10^{-6}$
  - $\underline{\Pi} = \nu_{\|} mn\left(\underline{\mathbf{I}} - 3\hat{\mathbf{b}}\hat{\mathbf{b}}\right)\hat{\mathbf{b}}\cdot\underline{\mathbf{W}}\cdot\hat{\mathbf{b}} - \nu_{iso} mn\underline{\mathbf{W}}\ ;\quad \nu_{\|} = 5\times 10^{-2},\quad \nu_{iso} = 5\times 10^{-5}$
- Artificial particle diffusivities are intended to be small. $\quad \underline{\mathbf{W}} = \nabla\mathbf{V} + \nabla\mathbf{V}^T - \frac{2}{3}\underline{\mathbf{I}}\nabla\cdot\mathbf{V}$
  - $D_n = 5\times 10^{-6}\ ,\quad D_h = 1\times 10^{-10}$
- NOTE: the equations used in this application have been normalized.
  - $\tau_A \equiv R_0^2 / F_{open} \cong 1;\quad \mu_0 \to 1,\quad n_0 \to 1$
  - $a \cong 0.8\ ;\quad R_0 = 1.6$

The edge of the initial profile is linearly unstable with a conducting wall.

- With the large edge resistivity and no flow, edge modes are unstable.

Growth rates computed for the initial equilibrium with conducting wall.

n	$\gamma\tau_A$
1	1.7×10^{-2}
2	-
3	1.8×10^{-3}
4	-

- Low-n growth rates increase only somewhat with a resistive wall with $v_{wall} = 1\times10^{-3}$.

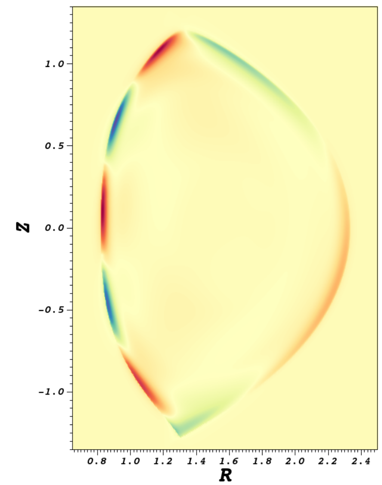

Peeling-type m = 4, n =1 mode is concentrated on the inboard side. (n = 1 pressure is shown.)

Robust asymmetric instability is a consequence of edge profile changes from wall contact.

- Edge profile changes are most evident from the axisymmetric computation.
- Loss of edge RB_ϕ and pressure enhances edge current.

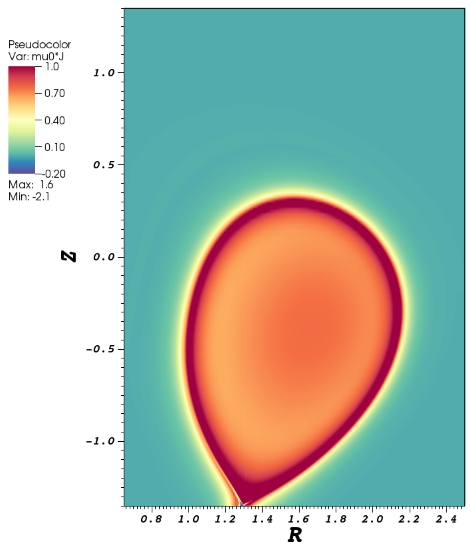

A strong current layer develops at the edge of the closed flux. [Plot shows $<\lambda>=<\mu_0 J_{||}/B>$ at t = 969.]

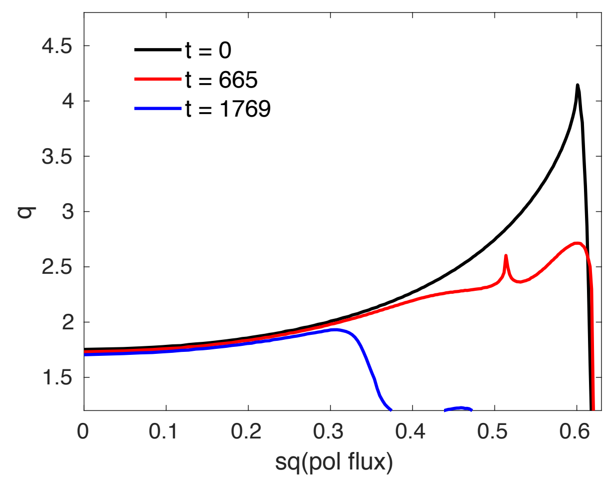

With increasing displacement, edge q is reduced.

The edge (3,1) distortion induces reversed parallel current ($\lambda = \mu_0 J_{||}/B$) at the plasma edge.

- This is inherent with radial displacement into poloidal flux and induces wall-current asymmetry [Zakharov, PoP **18**, 062503].
- The normal component of **J** has $O(1)$ toroidal variation.

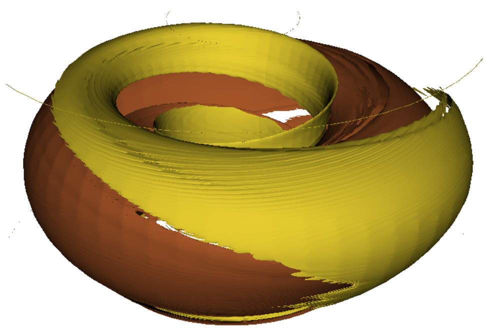

Isosurfaces of λ = -0.085 (mustard) and λ = +0.8 (brown) at t = 519. The negative region opposes the direction of plasma current.

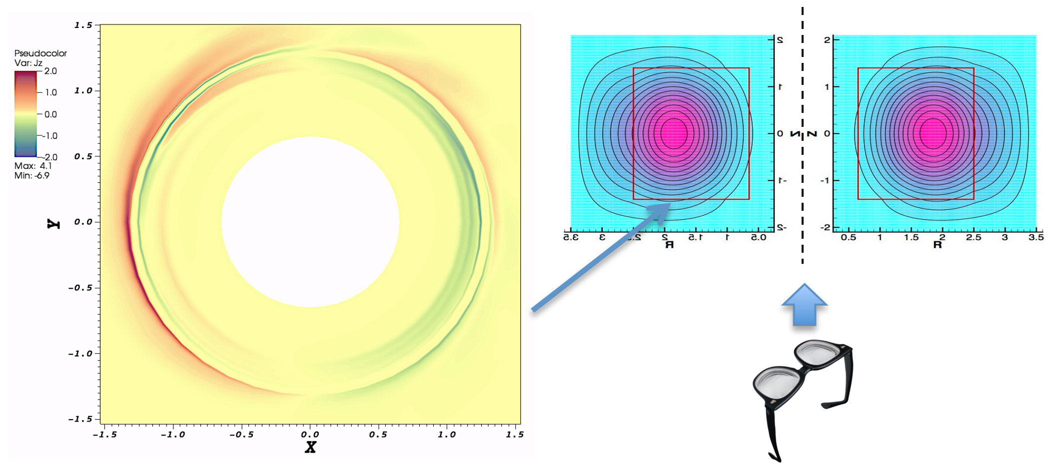

Contours of J_z just above the lower surface at t = 519, viewed from below.

We have used 2D computations to investigate sensitivity to boundary modeling.

- Two conditions on temperature have been tested.
  - T_{wall} is fixed at $T_0/10^4$ (used in 3D computation)
  - Insulating conditions
- Three conditions on flow-velocity have been tested.
  - Impenetrable, no-slip
  - Normal flow is $\mathbf{E}_{\text{wall}}\times\mathbf{B}$ drift using $\mathbf{E}_{\text{wall}}$ from resistive diffusion through the wall
  - Projection of local outward sonic flow along **B**
- Conditions on density at the wall have also been tested.
  - Fix $n_{wall} = 0.1 n_0$ with diffusion allowing particles to move through the wall
  - Allow normal flow to carry mass out

There is virtually no change when switching between impenetrable and drift-flow conditions on **V**.

- Ohm's law is non-ideal, so flux and perpendicular flow evolution are not frozen together.
- Changing the outward particle flux has moderate influence.

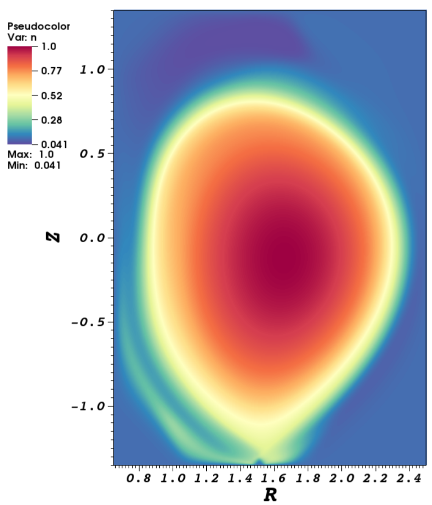

Particle density at t = 291 appears identical when changing V_{norm} alone.

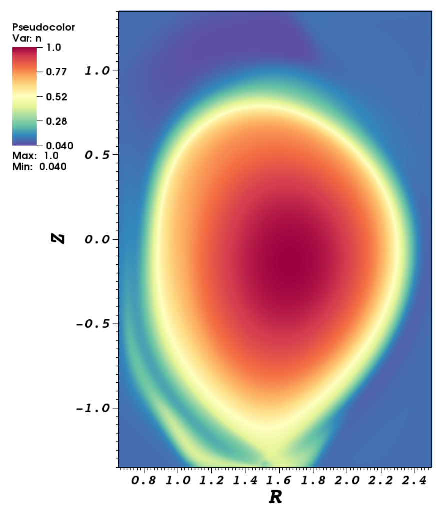

Limiting particle flux to be from flow (not diffusion) retains more mass.

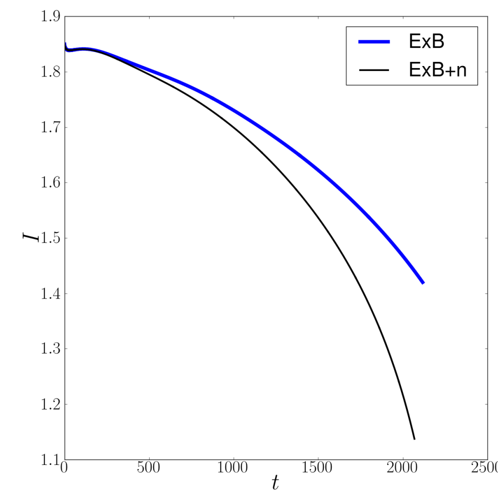

Plasma currents eventually deviate with different n BCs.

There is considerable sensitivity to heat flux modeling at the wall.

- Scrape-off occurs through edge cooling and its effect on $\eta(T)$ in the computations.
- Insulating conditions allow a broader halo-current layer and slow the evolution of I_p.

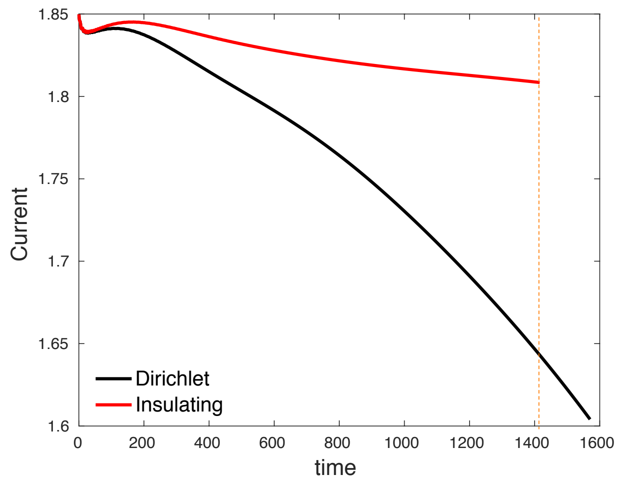

Evolution of plasma current is sensitive to boundary conditions on *T*.

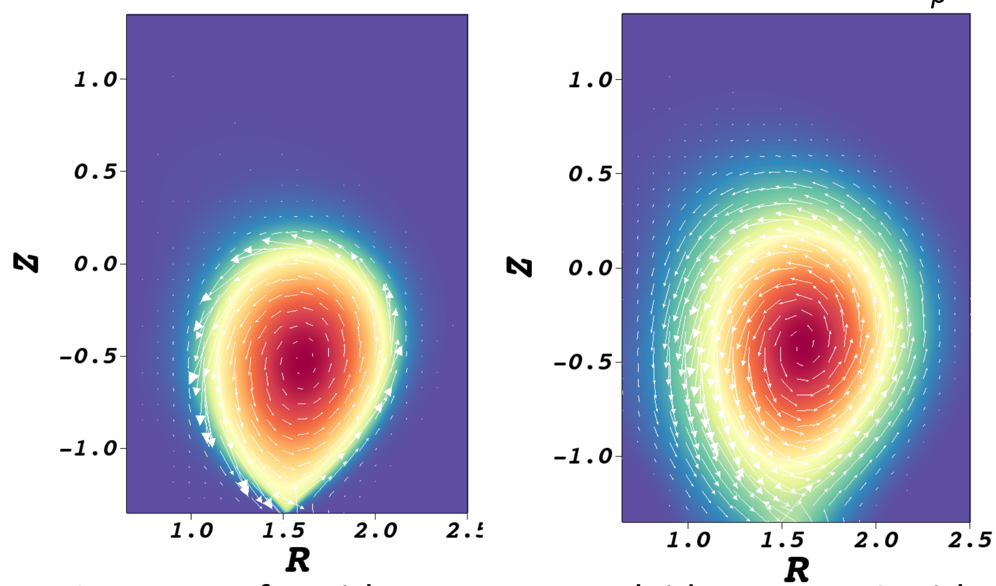

Contours of *T* with J vectors overlaid at t = 1410 with Dirichlet (left) and insulating (right).

We are developing more realistic boundary modeling by considering sheath effects.

- The boundary conditions derived for reduced turbulence modeling in [Loizu, *et al.*, Phys Plasmas **19**, 122307 (2012)] are based on conditions at the sheath/ magnetic pre-sheath interface.
- We are adapting these conditions for full-MHD and two-fluid computations.
  - Parallel flow is roughly the ion acoustic speed (at $T_i = 0$)
  - Tangential flow is from drifts, including sheath-**E**
  - Wall electrical potential varies along the surface
  - Parallel current is limited by what can be drawn (either ions or electrons, depending on potential drop across sheath)
  - Electrons are thermally insulated by the sheath (2-*T* modeling needed)